

1 **Improving β -galactosidase catalyzed transglycosylation yields by cross-linked**
2 **layer-by-layer enzyme immobilization**

3

4 Masih Karimi Alavijeh ^{a,b}, Anne S. Meyer ^c, Sally L. Gras ^{a,b}, Sandra E. Kentish ^{a,*}

5

6 ^a Department of Chemical Engineering, The University of Melbourne, Parkville, VIC

7 3010, Australia

8 ^b The Bio21 Molecular Science and Biotechnology Institute, The University of

9 Melbourne, Parkville, Vic 3010, Australia

10 ^c Protein Chemistry and Enzyme Technology Division, Department of Biotechnology

11 and Biomedicine, Technical University of Denmark, DTU, DK-2800, Kgs Lyngby,

12 Denmark

13

14

15

16 *Corresponding author:

17 E-mail: sandraek@unimelb.edu.au (Sandra Kentish).

18

19

20

21 **Abstract**

22 The biotransformation of lactose into gut-bioactive glycans catalyzed by β -
23 galactosidase can give economic value to lactose-rich side streams generated in the
24 food or dairy industry. Herein, we study the immobilization of the commercially used
25 β -galactosidase from *Bacillus circulans* onto silica particles using an enzyme
26 immobilization technology involving a cross-linked layer-by-layer encapsulation
27 method. The immobilized β -galactosidase was used for the synthesis of N-
28 acetyllactosamine (LacNAc) as an important precursor for numerous bioactive
29 compounds and a prebiotic in itself. Techniques including molecular analysis, enzyme
30 activity determination, secondary structure analysis, thermodynamic characterization
31 as well as the determination of thermal and operational stability were conducted to
32 characterize the immobilized enzyme. Changes in the activity of the enzyme after
33 immobilization were attributed to possible changes in electrostatic, covalent and
34 protein-protein interactions. Immobilization significantly improved enzymatic LacNAc
35 yield compared to the free enzyme. In turn, this improved the economics and the
36 sustainability of the process. The immobilized enzyme encapsulated in multilayer films
37 was significantly more stable in the presence of divalent cations and its thermostability
38 also substantially increased, with the thermal denaturation activation energy
39 increasing from 53 kJ mol⁻¹ to 294 kJ mol⁻¹. The immobilized enzyme was successfully
40 reused in eight consecutive reaction cycles with no significant reduction in the LacNAc
41 yield. The improved transgalactosylation yield and productivity, higher stability and

42 reusability obtained with this immobilization method provide new opportunities for
43 industrial applications.

44 **Keywords:** Layer-by-layer; Galacto-oligosaccharide; Enzyme; Immobilized β -
45 galactosidase; Stability; Silica.

46

47 INTRODUCTION

48 The global dairy industry produces large amounts of lactose-rich by-product
49 streams, particularly whey generated from manufacturing of cheese, casein and
50 yoghurt.¹⁻² Lactose valorization—the use of lactose in the synthesis of functional food
51 and pharmaceutical products—can enhance the economic and environmental
52 sustainability of the industry.^{1, 3} Although separation of proteins as a value-added
53 product from whey streams has become an established process over the past 30 years,
54 lactose valorization is still under development. Large amounts of the lactose generated
55 are not used and so regarded as low-value streams, imposing adverse environmental
56 impacts.^{1, 4-5} One solution to exploit this abundant resource is to synthesize lactose-
57 derived prebiotics, including galacto-oligosaccharides or human milk oligosaccharides,
58 via β -galactosidase-catalyzed transgalactosylation reactions. In a transgalactosylation
59 reaction, lactose typically acts as a galactosyl donor, which is cheaper and less toxic than
60 nitrophenyl glycosides.⁶⁻⁷

61 Glycosyltransferases can catalyze the formation of such prebiotics with very
62 high selectivity and high yields.⁸⁻⁹ Glycosyltransferases are not readily available,
63 however, making this process expensive. Further, most glycosyltransferases are also
64 incapable of undergoing variations in donor or acceptor. They act on an activated
65 nucleotide donor, which is unstable and expensive; the released nucleotide can also
66 strongly inhibit the action of these enzymes.⁹⁻¹⁰ In view of these limitations, the favored
67 enzymatic method for catalyzing transgalactosylation is based on the use of β -

68 galactosidases, which are able to act on lactose as the starting substrate. In this method,
69 however, hydrolysis of lactose can simultaneously be catalyzed in competition with
70 transgalactosylation, leading to lower yields and selectivity.

71 Different methods, including protein engineering,¹¹⁻¹² water activity reduction
72 ¹³⁻¹⁴ and optimization of operational parameters,¹⁵⁻¹⁶ have been developed by
73 researchers to increase the yield of transgalactosylation products in preference to
74 hydrolysis. In an alternative approach, enzyme immobilization has been shown to
75 improve the transgalactosylation efficiency in several studies.¹⁷⁻²⁰ Moreover,
76 immobilization increases the options for controlling the reaction (via reaction time
77 control) and eases enzyme separation and reuse after reaction, whilst also improving
78 the storage and operational enzyme stability.²¹ The thermal stability of β -
79 galactosidases often increases upon immobilization. This is a significant advantage for
80 transgalactosylation reactions, as at elevated temperatures higher concentrations of
81 starting substrates can be dissolved into solution, which favors transgalactosylation
82 relative to hydrolysis.^{7,22} The solubility of lactose is relatively low in aqueous solutions
83 at ambient temperatures, about 19 g per 100 g of water at 20 °C, whereas it is 60 g and
84 100 g per 100 g of water at 60 °C and 80 °C, respectively ²³ illustrating the large
85 potential gains that may be achieved at higher temperature.

86 Silica is widely used as a support material for enzyme immobilization, due to its
87 thermal and mechanical stability, microbial resistance and non-toxicity. Such silica
88 supports are commercially available and are easy to handle and synthesize.²⁴⁻²⁵

89 Electrostatic rather than Van der Waals forces are reported to be the main forces
90 governing adsorption of enzymes onto silica supports.²⁶⁻²⁷ Given the theoretical
91 isoelectric points of 3-4 and 4.5 for SiO₂²⁸⁻²⁹ and β-galactosidase,³⁰ respectively,
92 attractive electrostatic interactions between this enzyme and silica supports are not
93 likely to be very strong, especially at the optimum pH of β-galactosidase from *Bacillus*
94 *circulans* (pH=6), where both are negatively charged. This makes the enzyme more
95 susceptible to desorption from the support, which is problematic in terms of enzyme
96 reusability in successive cycles. This potential problem can be overcome by modifying
97 the silica surface using a chemical agent to activate the silanol groups on their surface.
98 Silanized SiO₂ can then be further treated by a cross-linker to prepare it for covalent
99 immobilization of an enzyme,³¹⁻³³ such as β-galactosidase.

100 Layer-by-layer assembly is another established method to encapsulate an enzyme and
101 to prevent its leakage from the support. In this technique, the adsorbed protein is
102 coated with oppositely charged polymers or polyelectrolytes. It is a simple and
103 extremely versatile technique for immobilization of various enzymes onto different
104 supports based on electrostatic interactions.³⁴ This method can be performed in
105 aqueous solutions under mild conditions, which is environmentally favorable and
106 reduces the likelihood of enzyme degradation. Furthermore, this method allows the co-
107 immobilization of multiple enzymes for cascade reactions.³⁵⁻³⁶ Enzyme covalent
108 immobilization on silicon substrates, on the other hand, involves in the use of
109 hazardous and toxic non-aqueous solutions such as organosilane reagents and toluene
110 with longer preparation times and a greater risk of enzyme denaturation.^{31, 37-38} Due to

111 the creation of very robust pairs with a high chemical and physical stability, polystyrene
112 sulfonate (PSS) and polyallylamine hydrochloride (PAH) have been widely employed in
113 layer-by-layer encapsulation methods, including the immobilization of enzymes.³⁹⁻⁴¹

114 While a number of workers have studied the covalent immobilization of β -
115 galactosidases for galactooligosaccharide production, no study has been performed to
116 analyze the effect of layer-by-layer immobilization on transglycosylation reactions.
117 Microenvironments and molecular interactions generated in multilayer films may
118 present some desirable impacts on the β -galactosidase enzyme stability and
119 hydrolysis/transgalactosylation activities. Hence, in the present study, we investigate
120 the suitability of a cross-linked layer-by-layer technique for the immobilization of β -
121 galactosidase derived from *Bacillus circulans*. Negatively charged silica particles are
122 first coated by the positively charged PAH followed by the electrostatic adsorption of
123 the negatively charged β -galactosidase, cross-linking with glutaraldehyde and
124 deposition of further PAH and PSS layers. In addition, for the first time, an analysis is
125 performed to analyze the economics and sustainability of such an immobilization
126 method.

127 **EXPERIMENTAL SECTION**

128 Sources of chemicals are provided in the Supporting Information as are detailed
129 descriptions of experimental protocols such as the hydrolytic assay.
130 transgalactosylation activity, determination of immobilization efficiency, activity

131 retention and thermal stability. Characterization methods and computational
132 molecular analysis are also described in the Supporting Information.

133 **Layer-by-layer adsorption of β -galactosidase onto SiO₂ particles**

134 Polyelectrolyte solutions of PSS or PAH (2 mg·ml⁻¹) were prepared in Tris buffer
135 (pH=7.2; 50 mM). The SiO₂ particles (SIPERNAT®)(50 mg) were dispersed in 1 ml of the
136 PAH solution. The suspension was mixed and sonicated using a water bath sonicator
137 (Ultrasonic Bath FXP4, 50 Hz, Ultrasonics, Australia) for 1 min. After 10 min shaking on
138 a tube rocker, the particles were collected by centrifugation at 7,000g for 1 min,
139 followed by re-suspension and vortex mixing in 1 ml Tris buffer (pH=7.2) to remove
140 free PAH and any impurities. This step was repeated three times, with the supernatant
141 discarded by centrifugation at 7,000g for 1 min after each rinsing. After the deposition
142 of this first layer of PAH, a total of 1 ml of the enzyme solution (0.1 mg·ml⁻¹) in
143 phosphate-citrate buffer (pH=6; 50 mM) was added to the tube containing the particles.
144 The adsorption of the enzyme took place for 20 min under mild shaking on a tube
145 rocker. The same procedure as already described for the free PAH removal was used to
146 collect and wash the particles and the supernatant as well as washings were collected
147 for measuring the un-adsorbed free enzyme. The immobilized enzyme was further
148 stabilized by cross-linking with 1 ml of 0.1% w/w glutaraldehyde solution at pH=7.2.
149 The solution containing 0.1% w/w glutaraldehyde in Tris buffer was made from a 25%
150 w/w glutaraldehyde stock solution. The excess glutaraldehyde was removed by
151 centrifugation and the particles were then washed three times.

152 In addition to the electrostatic interaction between the negatively charged β -
153 galactosidase with positively charged PAH, glutaraldehyde reacts with the amine
154 groups of PAH (and to a minor extent with exposed amine groups in the enzyme). Thus,
155 a subsequent layer of PAH was deposited on the particles as described earlier. The
156 particles were then exposed to 1 ml of PSS (2 mg·ml⁻¹) for 10 min followed by three
157 washings. The strong polyanionic PSS was used as the terminal layer as this
158 polyelectrolyte is more resistant to re-solubilization in comparison with a PAH layer.⁴²⁻
159 ⁴³ A schematic representation of this cross-linked layer-by-layer assembly is shown in
160 Figure 1.

161 For comparison, the enzyme was also pretreated by contact with lactose, as
162 there is evidence that this might protect the active site during the immobilization
163 process.⁴⁴ To this end, the enzyme solution (0.1 mg·ml⁻¹) was prepared in a phosphate-
164 citrate buffer (pH=6; 50 mM) containing 30 mM lactose. This solution was incubated at
165 37 °C for 1 h at 150 rpm before immobilization.⁴⁴

166 (Figure 1)

167 In all experiments, statistical significance was determined by the two-tail
168 Student's t-test (p<0.05) and all experimental data were indicated as mean value \pm one
169 standard deviation. Linear regression analysis (Excel Data Analysis ToolPak) was used
170 to determine the error associated with the regression line slope where needed. The
171 error propagation analysis was taken into account to calculate the overall error of a
172 parameter from the individual errors ⁴⁵.

173 RESULTS AND DISCUSSION

174 Characterization of the Immobilized Enzyme

175 The TGA thermograms (see Figure S1(B) in the Supporting Information) showed
176 a significantly greater mass loss upon heating from the silica particles with immobilized
177 enzyme compared to the bare silica supports. The mass loss below 200 °C is because of
178 dehydration.⁴⁶ The decomposition of the PAH side chains starts at around 230 °C
179 followed by the sulfonate groups in PSS.⁴⁷⁻⁴⁸ The loss at higher temperatures is
180 attributed to the degradation of the main polymeric backbones.⁴⁷⁻⁴⁹

181 Figure 2(A) shows the ATR-FTIR spectra of the native and immobilized enzyme.
182 The silica particles display a broad peak at 1,070 cm⁻¹ resulting from asymmetric
183 vibrations of Si-O.⁵⁰ The enzyme immobilization results in new peaks, particularly the
184 Amide I band (1,600 cm⁻¹ to 1,700 cm⁻¹) related to C-O stretching vibrations and the
185 Amide II band (1,510 cm⁻¹ to 1,580 cm⁻¹) related to N-H bending.⁵¹⁻⁵² New peaks
186 between 3,000 cm⁻¹ and 3,700 cm⁻¹ are indicative of N-H stretching and side chain
187 stretching.⁵³⁻⁵⁴ In addition, zeta potential measurements reveal surface charge
188 inversion, confirming the successful deposition of layers (Figure 2(B)).

189 The characteristic Amide I band is highly sensitive to small changes in molecular
190 geometry and hydrogen bond patterns and can be used to obtain more detailed
191 information on the secondary structure components of a protein.⁵⁵⁻⁵⁷ As shown in
192 Figure 2(C), the β -galactosidase enzyme immobilized using the cross-linked layer-by-
193 layer technique had an altered conformation. Changes in bands after immobilization

194 have been reported previously.⁵⁸⁻⁵⁹ Schwinté et al.⁶⁰ showed that encapsulating the
195 protein into the oppositely charged polyelectrolyte layers (PAH or PSS) can increase
196 the intermolecular β -sheet content. The enhanced protein-protein interactions are
197 associated with increased formation of intermolecular β -sheets, which can lead to
198 partial unfolding and denaturation.⁶¹⁻⁶² Such changes in the secondary structure of the
199 β -galactosidase may contribute to the modification of its catalytic activity.

200 (Figure 2)

201 **Evaluation of β -galactosidase hydrolytic activity after immobilization**

202 Layer-by-layer encapsulation of the β -galactosidase onto the SIPERNAT 50S
203 particles with an enzyme dosage of 2 mg per g silica resulted in a protein
204 immobilization efficiency of 100%. However, the hydrolytic enzyme activity after
205 immobilization was reduced to $22 \pm 2\%$. Such a reduction in activity is common during
206 immobilization due to interactions between the surface and enzyme, which can vary
207 depending on the immobilization method employed.⁶³ As shown in Figure 3,
208 electrostatic, covalent and protein-protein interactions might occur in the present case.
209 The positively charged PAH can interact with the enzyme at different locations, as the
210 enzyme is mainly negatively charged at pH=6, which is indicated by the red colour, with
211 some limited regions of positive charge shown in blue colour in Figure 3(A), leading to
212 the formation of polyelectrolyte-protein complexes.⁶⁴ The aldehyde groups in
213 glutaraldehyde can also form covalent bonds with free amine groups within the
214 enzyme, shown by a green colour in Figure 3(B). Covalent binding typically alters

215 enzyme activity.³² It has been reported that clusters or multilayers of the enzyme on
216 the support surface can be formed as a result of protein-protein interactions.^{63, 65} Figure
217 3(C) shows the protein-protein interaction sites (yellow regions) of the β -galactosidase
218 predicted by the PSIVER server. Protein-protein interactions dominate as greater initial
219 enzyme dosages are contacted with the support, resulting in a reduction in enzyme
220 activity due to steric hindrance and limited diffusion.^{32, 63, 65}

221 Increasing the enzyme dosage to 10 mg per g silica decreased the β -galactosidase
222 activity after immobilization to $17 \pm 2\%$, while all the enzyme protein was still adsorbed
223 by the support (see Table 1). A further increase in the enzyme dosage to $1000 \text{ mg}\cdot\text{g}^{-1}$
224 silica reduced the activity so that only $0.6 \pm 0.4\%$ of the free enzyme activity was
225 retained after immobilization. Further, the immobilization efficiency reduced to $22 \pm$
226 7% . In this case, the large increase in the amount of the enzyme loaded on the support
227 ($220 \pm 70 \text{ mg}\cdot\text{g}^{-1}$) led to a greater number of protein multilayers and interactions. Figure
228 3(D) shows the surface representation of the β -galactosidase with its surface catalytic
229 pocket region (cyan colour). According to this figure, the interactions described in
230 Figure 3(A-C) may block this region and hinder efficient access of the substrate to the
231 enzyme.

232

233

234

235 **Table 1.** Hydrolytic activity retention, immobilization efficiency and amount of
236 immobilized β -galactosidase adsorbed on the SIPERNAT 50S particles by the layer-by-
237 layer encapsulation method used in this study at different enzyme dosages.

Enzyme dosage (mg·g ⁻¹ silica)	Activity retention (%)	Immobilization efficiency (%)	Amount of immobilized enzyme (mg·g ⁻¹ silica)
2	22± 2	100	2
10	17 ± 2	100	10
30	13.5 ± 1.5	98.4 ± 0.6	29.5 ± 0.2
1000	0.6±0.4	22± 7	220 ± 70

238

239

240 We also examined the effect of lactose pre-treatment on the loss of enzyme
241 activity during the immobilization. It was reported that lactose binding to the active site
242 of β -galactosidase can act as a shield against the formation of covalent bonds near the
243 active site.⁴⁴ This protection method, however, did not result in any significant change
244 in the enzyme activity compared to the immobilized enzyme without lactose pre-
245 treatment. This result demonstrates that interactions other than covalent bonding play
246 a part in the change in enzyme conformation in this cross-linked layer-by-layer
247 assembly.

248

(Figure 3)

249 **Transgalactosylation reaction**

250 The immobilized biocatalyst with a load of 2 mg enzyme per g silica was then
251 used in the transgalactosylation reaction. Starting with the same initial hydrolytic
252 activities of 0.14 U·ml⁻¹ (corresponding to 40 µg·ml⁻¹ of the immobilized enzyme and 8
253 µg·ml⁻¹ of the free enzyme), the immobilized enzyme produced approximately two-fold
254 to three-fold more LacNAc compared to the free enzyme at each time point (Figure
255 4(A)). The ratio of initial transgalactosylation rate (r_{trans}) to hydrolysis rate (r_{hydro}) for
256 the immobilized enzyme is also about seven times greater than that for the free enzyme
257 (Figure 4(B)). Even when the free enzyme concentration is increased to 0.63 U·ml⁻¹
258 (corresponding to 36 µg·ml⁻¹ of the free enzyme), which is equivalent to the initial
259 transgalactosylation activity of the immobilized enzyme, the LacNAc production over
260 time did not reach to the same level as observed for the reaction with the immobilized
261 enzyme (Figure 4(A)), due to competition from the hydrolysis reaction. This is an
262 important result, which shows that the immobilization technique employed in this
263 study not only makes it possible to recover the enzyme after the reaction but also that
264 immobilization increases yield, which can significantly influence the economy of large-
265 scale LacNAc production.²

266 For further elucidation, as shown in Figure 4(C), the reaction specific
267 productivity (also known as biocatalytic productivity rate) was calculated at two time
268 points when the highest LacNAc concentrations were obtained in the reactions
269 catalyzed by the free enzyme at 0.63 U·ml⁻¹ (90 min) and the immobilized enzyme at
270 0.14 U·ml⁻¹ (150 min), respectively. When the free enzyme is used, a greater amount of

271 LacNAc can be achieved using $0.63 \text{ U}\cdot\text{ml}^{-1}$ rather than $0.14 \text{ U}\cdot\text{ml}^{-1}$ but at the expense of
272 a reduction in the specific productivity. In contrast, the specific productivity of the
273 reaction catalyzed by $0.14 \text{ U}\cdot\text{ml}^{-1}$ of the immobilized enzyme is greater than that of the
274 reaction run by $0.63 \text{ U}\cdot\text{ml}^{-1}$ of the free enzyme for either time point. The higher specific
275 productivity of $0.14 \text{ U}\cdot\text{ml}^{-1}$ of the free enzyme is due to the lower enzyme mass
276 concentration ($8 \mu\text{g}\cdot\text{ml}^{-1}$) of the immobilized enzyme ($40 \mu\text{g}\cdot\text{ml}^{-1}$) at the same
277 hydrolytic activity. Nonetheless, the ability to re-use the immobilized enzyme may
278 compensate for the loss of activity. Changes in the transgalactosylation yield and
279 reaction productivity upon immobilization of β -galactosidases have been reported by
280 several researchers.^{17, 66-68}

281 As previously shown,⁶⁹ high concentrations of divalent cations, i.e. 100 mM Ca^{2+}
282 or 100 mM Mg^{2+} can lead to the formation of salt bridges between the negatively
283 charged β -galactosidases and subsequent protein aggregation. Thus, in the present
284 study, we also examined the effect of these cations on the product formation when the
285 immobilized enzyme is used. As can be seen in Figure 4(A), no significant change in the
286 concentration of LacNAc in the presence of 100 mM Ca^{2+} or 100 mM Mg^{2+} is observed. This result
287 indicates that the enzyme is well encapsulated into the support and is unable to form
288 aggregates with neighbouring molecules. It also confirms our previous conclusion that
289 these cations have no role as co-factors of this enzyme.

290 (Figure 4)

291 In our previous work,⁶⁹ we developed a kinetic model to describe the multi-
292 pathway reactions including transgalactosylation and hydrolysis involved in the
293 conversion of lactose to LacNAc. Based on this model (see the Supporting Information),
294 the reaction rate constants were estimated for the free enzyme and the immobilized
295 enzyme (Table S1). The altered kinetic parameters are indicative of changes in the
296 catalytic active site and/or the restriction on substrate diffusion into the layer-by-layer
297 coating, which decreases the reaction rate constants after immobilization.⁷⁰⁻⁷¹
298 Importantly, the ratio of the LacNAc synthesis rate constant (k_3) to galactose release
299 rate constant (k_2) is 14 M^{-1} for the free enzyme while that for the immobilized enzyme
300 is about 20 M^{-1} , which demonstrates improved transgalactosylation.

301 **Thermal stability of the immobilized enzyme versus free enzyme**

302 The immobilized enzyme could retain about 92% and 83% of its initial activity
303 after 90 min and 180 min at $55 \text{ }^\circ\text{C}$, respectively (Figure 5(A)), while only 8% of the
304 initial activity of the free enzyme was maintained after 30 min (Figure 5(B)). This
305 means that with an immobilized enzyme it is possible to run reactions at elevated
306 temperature and thus at a higher reaction rate. At even higher temperatures, the
307 immobilized enzyme begins to denature more rapidly (Figure 5(C)), so that at 70°C , the
308 residual activity is more comparable (7% for the free enzyme and 15% for the
309 immobilized after 15 minutes). This observation is consistent with the inactivation rate
310 constant (k_D) data shown in Table 2. However even at 70°C , the immobilized enzyme
311 remains more thermally robust.

312 **Table 2.** Inactivation rate constant (k_D), half-time values ($t_{1/2}$) and activation energy of
 313 thermal denaturation reaction (E_a) for the immobilized and free enzyme.

T (°C)	$k_D \times 10^3$ (min ⁻¹)			$t_{1/2}$ (min)		
	Free enzyme	Immobilized enzyme	Two-tailed p-value	Free enzyme	Immobilized enzyme	Two-tailed p-value
55	77 ± 9	1.2 ± 0.3	5×10 ⁻⁸	9 ± 1	580 ± 140	3×10 ⁻¹⁰
60	96 ± 7	6 ± 0.5	3×10 ⁻⁹	7 ± 0.4	117 ± 9	2×10 ⁻²²
65	142 ± 13	33 ± 2	4×10 ⁻⁶	5 ± 0.4	21 ± 1	5×10 ⁻¹⁷
70	174 ± 10	127 ± 18	2×10 ⁻⁵	4 ± 0.2	5 ± 1	2×10 ⁻²
E_a (kJ mol⁻¹)						
Free enzyme			Immobilized enzyme			
53 ± 1			294 ± 2			

314

315

(Figure 5)

316 The activation energy (E_a) for the thermal denaturation reaction, or the
 317 minimum energy needed for triggering enzyme inactivation, is 53 ± 1 kJ mol⁻¹ for the
 318 free enzyme and 294 ± 2 kJ mol⁻¹ for the immobilized enzyme (Table 2). The higher E_a
 319 of the immobilized enzyme, which is more than five-fold that of the free enzyme,
 320 corroborates the suitability of the cross-linked layer-by-layer immobilization technique
 321 as a method for improving the thermal stability of β -galactosidase.

322

323 The positive ΔS observed for the immobilized enzyme (Table 3) is directly
324 indicative of protein unfolding (greater disorder) during inactivation.⁷²⁻⁷³ By contrast,
325 the corresponding negative ΔS values for the free enzyme can be related to the
326 formation of protein aggregates during inactivation as a result of denaturation. The
327 aggregates are less disordered compared to the soluble proteins moving freely in the
328 solution, hence the negative ΔS values.⁷⁴⁻⁷⁵

329 The positive values of ΔH indicate that thermal inactivation of the β -
330 galactosidase is an endothermic reaction, and the differences in the ΔH values of the
331 free vs the immobilized enzyme implies that more energy required to destabilize the
332 immobilized form (Table 3). The formation of an electrostatic cage as a result of the
333 interaction between the enzyme and polyelectrolytes can restrict structural
334 fluctuations, leading to improved structural stability within the protein.⁶⁰ It has been
335 demonstrated that a greater β -sheet content in a protein also leads to a more rigid
336 protein structure.⁷⁶ As described above, the FTIR spectra of the immobilized enzyme is
337 consistent with such changes in secondary structure confirmation and the formation of
338 a more rigid structure following immobilization.⁵⁹

339

340 **Table 3.** Thermodynamic parameters of thermal inactivation of the immobilized and
341 free enzyme.

T (°C)	ΔH (kJ mol ⁻¹)		ΔS (J mol ⁻¹ K ⁻¹)	
	Free enzyme	Immobilized enzyme	Free enzyme	Immobilized enzyme
55	50 ±1	291 ±2	-148 ± 4	552 ± 6
60	50 ±1	291 ±2	-149 ± 4	551 ± 0.7
65	50 ±1	291 ±2	-148 ± 4	552±0.5
70	50 ±1	291 ±2	-149 ± 4	551 ± 1

342

343

344 The immobilized enzyme and free enzyme were also incubated at these elevated
345 temperatures for 30 min and the remaining transgalactosylation activity then
346 measured at 50 °C. The transgalactosylation activity of the immobilized enzyme
347 incubated at 55 °C was unchanged, while around 86% of this activity was retained after
348 incubating the immobilized enzyme at 60 °C (Figure 6). A much more significant
349 decrease in activity was observed for the free enzyme after incubation at temperatures
350 higher than the optimum temperature of this β -galactosidase (50 °C).

351

(Figure 6)

352

374 same initial transgalactosylation activities; $0.14 \text{ U}\cdot\text{ml}^{-1}$ ($40 \mu\text{g}\cdot\text{ml}^{-1}$) for the immobilized
375 case and $0.63 \text{ U}\cdot\text{ml}^{-1}$ ($36 \mu\text{g}\cdot\text{ml}^{-1}$) for the free enzyme. The cost of immobilizing the
376 enzyme at a production scale was estimated as \$104 per kg of the immobilized support,
377 based on the calculations and process flowsheet of unit operations shown in the
378 Supporting Information (Figure S3). Other assumptions and economic parameters used
379 in the simulation are shown in Table S2.

380 The annual cost of raw materials per kg of product is 149 US dollars for the process
381 based on the immobilized enzyme with eight reuse cycles, while it is 178 US dollars for
382 the process based on the free enzyme (Table 4). This difference reflects the greater yield
383 obtained when using the immobilized enzyme. As shown in Figure S4 in the Supporting
384 Information, with no reuse of the immobilized biocatalyst, 72% of the total raw material
385 costs arises from the immobilization of the enzyme, whereas the share of the free
386 enzyme cost in the total raw material costs is about 19%. This finding is in agreement
387 with previously reported results.⁷⁷ As the number of reuse cycles increases, however,
388 this share falls, so that these costs are comparable after 11 reuse cycles.

389 The Net Present Value (NPV) was then calculated as an indicator of the project
390 profitability (see Supporting Information). The NPV for the plant processing 20 tons of
391 lactose per year based on the immobilized enzyme (463 million US dollars) is greater
392 than that for the process based on the free enzyme (333 million US dollars). This
393 increase in the NPV is mainly due to the increase in the yield after immobilization. As
394 shown in Figure 4(A), starting with the same initial transgalactosylation activities and

395 a lactose concentration of 50 mM, the molar yield of LacNAc is about 50% when the
396 immobilized enzyme is used, versus 35% for the free enzyme. For both enzyme types,
397 the process costs are close to each other, as no change in the equipment sizes occurs
398 (Table S2 in the Supporting Information), although there is an additional cost for
399 immobilization that is included for this case. Nonetheless, in each batch more LacNAc
400 is produced with the same amount of lactose when the immobilized enzyme is used,
401 indicating a higher annual revenue. Further analysis of the effect of the immobilized
402 enzyme reuse on the NPV is also shown in Figure 7(B). According to this figure,
403 variations in the NPV values are significant as the number of reuses increases up to
404 about 10. Further increases in the NPV are not very significant for higher reuse
405 numbers assuming the yield of product does not change.

406 The sustainability of the process based on the immobilized enzyme with eight reuse
407 cycles and free enzyme is further outlined in Table 4. The water used in the wash cycles
408 of the enzyme immobilization process can be recycled for the production of fresh
409 polyelectrolyte and enzyme solutions, so a 90% water recovery is assumed. As the
410 immobilized enzyme can be recycled at least eight times, the net water usage becomes
411 small, only 14 kg per kg LacNAc. The net electricity usage from the centrifugation in this
412 immobilization process is also low (0.004 kWh per kg LacNAc). Recycling of the
413 immobilized enzyme within the LacNAc reactor requires an additional filtration and
414 washing process and this also increases the total waste generated and water consumed
415 per kg of product. Nonetheless, it can be assumed that most of the water from this wash

416 step can be recycled to the reactor and so a water recovery of 90% is again used for this
417 step.

418 The use of the immobilized enzyme results in a lower chemical oxygen demand
419 (COD) per kg of product. In turn, this reduces the CO₂ equivalent emissions per kg of
420 LacNAc in the subsequent wastewater treatment processes, when emission factors for
421 either an aerobic or anaerobic treatment are applied.⁷⁸ The electricity, steam and
422 chilled water consumption also fall, which will further reduce CO₂ emissions if these
423 utilities are supplied using a fossil fuel energy source. Further, the amount of chemical
424 agents used in Clean-In-Place (CIP) for cleaning equipment is 354 kg per kg LacNAc
425 when the immobilized enzyme is applied, while 440 kg of these agents per kg LacNAc
426 are needed when the free enzyme is utilized. The reduction in these chemicals will
427 further reduce the environmental impact.

428

429

430

431

432 **Table 4.** Evaluation of the process sustainability based on either the free enzyme; or
 433 the immobilized enzyme with eight reuse cycles.

Sustainability Parameter	Units	Quantity per kg product for:	
		Free enzyme	Immobilized enzyme
Waste	kg	582	486
Total chemical oxygen demand (COD)	kg	10	8
Emission from waste ¹			
- Anaerobic treatment or:	kg CO ₂	10	8
- Aerobic treatment	equivalents	23	18
Raw materials	kg	210	188
Cleaning-In-Place (CIP) solutions ²	kg	440	354
Water consumption	kg	201	181
Electricity	kWh	3	2
Steam	kg	338	265
Chilled water	tonne	23	18
Raw material cost	USD	178	149
Waste treatment cost	USD	0.32	0.28
Utility cost	USD	11	9
Labor-dependent cost	USD	499	408
CIP cost	USD	21	17

¹ Emission factors of 1 kg CO₂eq.kg⁻¹ COD for anaerobic treatment and 2.4 kg CO₂eq.kg⁻¹ COD for aerobic treatment were assumed.⁷⁸

² Water rinse (WFI: water for injection), caustic rinse (0.5 M NaOH) and acid rinse (5% w/w H₃PO₄).

434

435

436

437 **Conclusions**

438 In this work, we have demonstrated that cross-linked layer-by-layer encapsulation
439 of β -galactosidase enzyme derived from *Bacillus circulans* can effectively improve the
440 transgalactosylation activity, whilst also improving stability and enabling reuse of the
441 enzyme. An enzyme dosage of 2 mg per g support resulted in an immobilization
442 efficiency of 100% with 21.5% of hydrolytic activity retained. Molecular analysis
443 indicates a range of different interactions during immobilization that may be associated
444 with the loss of enzyme activity. Further increase in the initial enzyme dosage resulted
445 in greater protein-protein interactions, leading to a more severe loss of activity. The
446 immobilized enzyme produced more LacNAc in comparison with the free enzyme at the
447 same hydrolytic activity. This can be attributed to conformational changes observed by
448 spectroscopy. The free enzyme was thermally unstable at 55 °C, losing 92% of its initial
449 activity after 30 min, while the immobilized counterpart was significantly more
450 thermostable and for instance retained 92% of its initial activity after 90 min at 55 °C.
451 The enhanced thermal stability and strong retention of the enzyme on the silica support
452 facilitated the reuse of the enzyme for at least eight successive cycles with no significant
453 reduction in the LacNAc yield. The enhanced yield at the same initial
454 transgalactosylation activity led to a significantly greater economic value for LacNAc
455 production, based on simulation results. The simulations also indicate that the use of
456 an immobilized enzyme would lead to reduced greenhouse gas emissions and reduced
457 need for wastewater treatment facilities. These enhancements in conjunction with the

458 use of a commercially available silica support meet the essential requirements for large-
459 scale application.

460 **Acknowledgements**

461 M. Karimi Alavijeh acknowledges The University of Melbourne for a Melbourne
462 Research Scholarship.

463

464 **Supporting Information**

465 The Supporting Information is available online free of charge.

466 Materials and methods; estimated rate constants for the free and immobilized
467 enzymes; assumptions and economic parameters used for economic evaluations;
468 raw materials and utility costs; TGA of silica before and after enzyme
469 immobilization; calculated time-course variations in sugar concentrations based on
470 the kinetic model; a schematic representation of the unit operations for
471 immobilizing the enzyme; changes in the share of the total raw material cost that
472 arises from enzyme immobilization versus the number of reuse cycles.

473

474 **References**

475 (1) Andler, S. M.; Goddard, J. M., Transforming food waste: how immobilized enzymes
476 can valorize waste streams into revenue streams. *NPJ Sci. Food* **2018**, *2*, 19-19, DOI:
477 10.1038/s41538-018-0028-2.

478 (2) Karimi Alavijeh, M.; Meyer, A. S.; Gras, S. L.; Kentish, S. E., Simulation and economic
479 assessment of large-scale enzymatic N-acetyllactosamine manufacture. *Biochem. Eng. J.*
480 **2020**, *154*, 107459, DOI: 10.1016/j.bej.2019.107459.

- 481 (3) Gänzle, M. G., Chapter 4 - Lactose—a conditional prebiotic? In *Lactose*, Paques, M.;
482 Lindner, C., Eds. Academic Press: 2019; pp 155-173.
- 483 (4) Tavares, T.; Malcata, F. X., Whey and Whey Powders: Fermentation of Whey. In
484 *Encyclopedia of Food and Health*, Caballero, B.; Finglas, P. M.; Toldrá, F., Eds. Academic
485 Press: Oxford, 2016; pp 486-492.
- 486 (5) Boland, M., 3 - Whey proteins. In *Handbook of Food Proteins*, Phillips, G. O.; Williams,
487 P. A., Eds. Woodhead Publishing: 2011; pp 30-55.
- 488 (6) Zeuner, B.; Jers, C.; Mikkelsen, J. D.; Meyer, A. S., Methods for Improving Enzymatic
489 Trans-glycosylation for Synthesis of Human Milk Oligosaccharide Biomimetics. *J. Agric.*
490 *Food Chem.* **2014**, *62* (40), 9615-9631, DOI: 10.1021/jf502619p.
- 491 (7) Gosling, A.; Stevens, G. W.; Barber, A. R.; Kentish, S. E.; Gras, S. L., Recent advances
492 refining galactooligosaccharide production from lactose. *Food Chem.* **2010**, *121* (2),
493 307-318, DOI: 10.1016/j.foodchem.2009.12.063.
- 494 (8) Downey, A. M.; Hocek, M., Strategies toward protecting group-free glycosylation
495 through selective activation of the anomeric center. *Beilstein J. Org. Chem.* **2017**, *13*,
496 1239-1279, DOI: 10.3762/bjoc.13.123.
- 497 (9) Seeberger, P.; Finney, N.; Rabuka, D., Chemical and Enzymatic Synthesis of Glycans
498 and Glycoconjugates. In *Essentials of Glycobiology. 2nd edition*, Varki, A.; Cummings, R.;
499 Esko, J., Eds. Cold Spring Harbor Laboratory Press: NY, 2009.
- 500 (10) Wang, Z. A.; van der Wel, H.; Vohra, Y.; Buskas, T.; Boons, G. J.; West, C. M., Role
501 of a cytoplasmic dual-function glycosyltransferase in O₂ regulation of development in
502 *Dictyostelium*. *J Biol Chem* **2009**, *284* (42), 28896-904, DOI: 10.1074/jbc.M109.022574.
- 503 (11) Qin, Z.; Li, S.; Huang, X.; Kong, W.; Yang, X.; Zhang, S.; Cao, L.; Liu, Y., Improving
504 Galactooligosaccharide Synthesis Efficiency of β -Galactosidase Bgal1-3 by Reshaping
505 the Active Site with an Intelligent Hydrophobic Amino Acid Scanning. *J. Agric. Food*
506 *Chem.* **2019**, *67* (40), 11158-11166, DOI: 10.1021/acs.jafc.9b04774.
- 507 (12) Lundemo, P.; Adlercreutz, P.; Karlsson, E. N., Improved Transferase/Hydrolase
508 Ratio through Rational Design of a Family 1 β -Glucosidase from *Thermotoga*

- 509 neapolitana. *Appl. Environ. Microbiol.* **2013**, 79 (11), 3400, DOI: 10.1128/AEM.00359-
510 13.
- 511 (13) Gosling, A.; Stevens, G. W.; Barber, A. R.; Kentish, S. E.; Gras, S. L., Effect of the
512 Substrate Concentration and Water Activity on the Yield and Rate of the Transfer
513 Reaction of β -Galactosidase from *Bacillus circulans*. *J. Agric. Food Chem.* **2011**, 59 (7),
514 3366-3372, DOI: 10.1021/jf104397w.
- 515 (14) Kwon, S. J.; Jung, H.-C.; Pan, J.-G., Transgalactosylation in a Water-Solvent
516 Biphasic Reaction System with β -Galactosidase Displayed on the Surfaces of Spores.
517 *Appl. Environ. Microbiol.* **2007**, 73 (7), 2251, DOI: 10.1128/AEM.01489-06.
- 518 (15) González-Delgado, I.; López-Muñoz, M.-J.; Morales, G.; Segura, Y., Optimisation of
519 the synthesis of high galacto-oligosaccharides (GOS) from lactose with β -galactosidase
520 from *Kluyveromyces lactis*. *Int. Dairy J.* **2016**, 61, 211-219, DOI:
521 10.1016/j.idairyj.2016.06.007.
- 522 (16) Carević, M.; Veličković, D.; Stojanović, M.; Milosavić, N.; Rogniaux, H.; Ropartz, D.;
523 Bezbradica, D., Insight in the regioselective enzymatic transgalactosylation of salicin
524 catalyzed by β -galactosidase from *Aspergillus oryzae*. *Process Biochem.* **2015**, 50 (5),
525 782-788, DOI: 10.1016/j.procbio.2015.01.028.
- 526 (17) Guerrero, C.; Aburto, C.; Suárez, S.; Vera, C.; Illanes, A., Effect of the type of
527 immobilization of β -galactosidase on the yield and selectivity of synthesis of
528 transgalactosylated oligosaccharides. *Biocatal. Agric. Biotechnol.* **2018**, 16, 353-363,
529 DOI: 10.1016/j.bcab.2018.08.021.
- 530 (18) Sen, D.; Sarkar, A.; Gosling, A.; Gras, S. L.; Stevens, G. W.; Kentish, S. E.;
531 Bhattacharya, P. K.; Barber, A. R.; Bhattacharjee, C., Feasibility study of enzyme
532 immobilization on polymeric membrane: A case study with enzymatically galacto-
533 oligosaccharides production from lactose. *J. Membr. Sci.* **2011**, 378 (1), 471-478, DOI:
534 10.1016/j.memsci.2011.05.032.
- 535 (19) Mozaffar, Z.; Nakanishi, K.; Matsuno, R., Effect of glutaraldehyde on
536 oligosaccharide production by β -galactosidase from *Bacillus circulans*. *Appl. Microbiol.*
537 *Biotechnol.* **1987**, 25 (5), 426-429, DOI: 10.1007/BF00253312.

- 538 (20) Misson, M.; Du, X.; Jin, B.; Zhang, H., Dendrimer-like nanoparticles based β -
539 galactosidase assembly for enhancing its selectivity toward transgalactosylation.
540 *Enzyme Microb. Technol.* **2016**, *84*, 68-77, DOI: 10.1016/j.enzmictec.2015.12.008.
- 541 (21) Panesar, P. S.; Kumari, S.; Panesar, R., Potential Applications of Immobilized β -
542 Galactosidase in Food Processing Industries. *Enzyme Res.* **2010**, *2010*, 473137-473137,
543 DOI: 10.4061/2010/473137.
- 544 (22) Zeuner, B.; Nyffenegger, C.; Mikkelsen, J. D.; Meyer, A. S., Thermostable β -
545 galactosidases for the synthesis of human milk oligosaccharides. *New Biotechnol.* **2016**,
546 *33* (3), 355-360, DOI: 10.1016/j.nbt.2016.01.003.
- 547 (23) Fox, P. F., Lactose: Chemistry and Properties. In *Advanced Dairy Chemistry:*
548 *Volume 3: Lactose, Water, Salts and Minor Constituents*, McSweeney, P.; Fox, P. F., Eds.
549 Springer New York: New York, NY, 2009; pp 1-15.
- 550 (24) Bhatia, R. B.; Brinker, C. J.; Gupta, A. K.; Singh, A. K., Aqueous Sol-Gel Process for
551 Protein Encapsulation. *Chem. Mater.* **2000**, *12* (8), 2434-2441, DOI:
552 10.1021/cm000260f.
- 553 (25) Bernal, C.; Sierra, L.; Mesa, M., Design of β -galactosidase/silica biocatalysts:
554 Impact of the enzyme properties and immobilization pathways on their catalytic
555 performance. *Eng. Life Sci.* **2014**, *14* (1), 85-94, DOI: 10.1002/elsc.201300001.
- 556 (26) Hüttner, S.; Zezzi Do Valle Gomes, M.; Iancu, L.; Palmqvist, A.; Olsson, L.,
557 Immobilisation on mesoporous silica and solvent rinsing improve the
558 transesterification abilities of feruloyl esterases from *Myceliophthora thermophila*.
559 *Bioresour. Technol.* **2017**, *239*, 57-65, DOI: 10.1016/j.biortech.2017.04.106.
- 560 (27) Deere, J.; Magner, E.; Wall, J. G.; Hodnett, B. K., Mechanistic and Structural
561 Features of Protein Adsorption onto Mesoporous Silicates. *J. Phys. Chem. B* **2002**, *106*
562 (29), 7340-7347, DOI: 10.1021/jp0139484.
- 563 (28) Essa, H.; Magner, E.; Cooney, J.; Hodnett, B. K., Influence of pH and ionic strength
564 on the adsorption, leaching and activity of myoglobin immobilized onto ordered
565 mesoporous silicates. *J. Mol. Catal. B Enzym.* **2007**, *49* (1), 61-68, DOI:
566 10.1016/j.molcatb.2007.07.005.

- 567 (29) Givens, B. E.; Diklich, N. D.; Fiegel, J.; Grassian, V. H., Adsorption of bovine serum
568 albumin on silicon dioxide nanoparticles: Impact of pH on nanoparticle-protein
569 interactions. *Biointerphases* **2017**, *12* (2), 02D404-02D404, DOI: 10.1116/1.4982598.
- 570 (30) Food Standards Australia & New Zealand *β -galactosidase derived from *Bacillus**
571 *circulans as a processing aid*; Food Standards Australia & New Zealand: 2012.
- 572 (31) Eskandarloo, H.; Abbaspourrad, A., Production of galacto-oligosaccharides from
573 whey permeate using β -galactosidase immobilized on functionalized glass beads. *Food*
574 *Chem.* **2018**, *251*, 115-124, DOI: 10.1016/j.foodchem.2018.01.068.
- 575 (32) Zeuner, B.; González-Delgado, I.; Holck, J.; Morales, G.; López-Muñoz, M.-J.;
576 Segura, Y.; Meyer, A. S.; Mikkelsen, J. D., Characterization and immobilization of
577 engineered sialidases from *Trypanosoma rangeli* for transsialylation. *AIMS Mol. Sci.*
578 **2017**, *4* (2), 140-163, DOI: <http://dx.doi.org/10.3934/molsci.2017.2.140>.
- 579 (33) Song, Y.-S.; Lee, H.-U.; Park, C.; Kim, S.-W., Optimization of lactulose synthesis
580 from whey lactose by immobilized β -galactosidase and glucose isomerase. *Carbohydr.*
581 *Res.* **2013**, *369*, 1-5, DOI: 10.1016/j.carres.2013.01.002.
- 582 (34) Zhao, S.; Caruso, F.; Dähne, L.; Decher, G.; De Geest, B. G.; Fan, J.; Feliu, N.; Gogotsi,
583 Y.; Hammond, P. T.; Hersam, M. C.; Khademhosseini, A.; Kotov, N.; Leporatti, S.; Li, Y.;
584 Lisdat, F.; Liz-Marzán, L. M.; Moya, S.; Mulvaney, P.; Rogach, A. L.; Roy, S.; Shchukin, D.
585 G.; Skirtach, A. G.; Stevens, M. M.; Sukhorukov, G. B.; Weiss, P. S.; Yue, Z.; Zhu, D.; Parak,
586 W. J., The Future of Layer-by-Layer Assembly: A Tribute to ACS Nano Associate Editor
587 Helmuth Möhwald. *ACS Nano* **2019**, *13* (6), 6151-6169, DOI:
588 10.1021/acsnano.9b03326.
- 589 (35) Sakr, O. S.; Borchard, G., Encapsulation of Enzymes in Layer-by-Layer (LbL)
590 Structures: Latest Advances and Applications. *Biomacromolecules* **2013**, *14* (7), 2117-
591 2135, DOI: 10.1021/bm400198p.
- 592 (36) Feifel, S. C.; Kapp, A.; Lisdat, F., Protein Multilayer Architectures on Electrodes
593 for Analyte Detection. In *Biosensors Based on Aptamers and Enzymes*, Gu, M. B.; Kim, H.-
594 S., Eds. Springer Berlin Heidelberg: Berlin, Heidelberg, 2014; pp 253-298.
- 595 (37) Gunda, N. S. K.; Singh, M.; Norman, L.; Kaur, K.; Mitra, S. K., Optimization and
596 characterization of biomolecule immobilization on silicon substrates using (3-

- 597 aminopropyl)triethoxysilane (APTES) and glutaraldehyde linker. *Appl. Surf. Sci.* **2014**,
598 *305*, 522-530, DOI: 10.1016/j.apsusc.2014.03.130.
- 599 (38) Bernal, C.; Urrutia, P.; Illanes, A.; Wilson, L., Hierarchical meso-macroporous
600 silica grafted with glyoxyl groups: opportunities for covalent immobilization of
601 enzymes. *New Biotechnol.* **2013**, *30* (5), 500-506, DOI: 10.1016/j.nbt.2013.01.011.
- 602 (39) Reurink, D. M.; te Brinke, E.; Achterhuis, I.; Roesink, H. D. W.; de Vos, W. M.,
603 Nafion-Based Low-Hydration Polyelectrolyte Multilayer Membranes for Enhanced
604 Water Purification. *ACS Appl. Polym. Mater.* **2019**, *1* (9), 2543-2551, DOI:
605 10.1021/acsapm.9b00689.
- 606 (40) Godoy-Gallardo, M.; Labay, C.; Hosta-Rigau, L., Tyrosinase-Loaded
607 Multicompartment Microreactor toward Melanoma Depletion. *ACS Appl. Mater.*
608 *Interfaces* **2019**, *11* (6), 5862-5876, DOI: 10.1021/acsami.8b20275.
- 609 (41) Kozlovskaya, V.; Kharlampieva, E.; Sukhishvili, S. A., 1.25 Polymer Films Using
610 LbL Self-Assembly. In *Comprehensive Biomaterials II*, Ducheyne, P., Ed. Elsevier: Oxford,
611 2017; pp 554-569.
- 612 (42) Adamczyk, Z.; Zembala, M.; Warszyński, P.; Jachimska, B., Characterization of
613 Polyelectrolyte Multilayers by the Streaming Potential Method. *Langmuir* **2004**, *20*
614 (24), 10517-10525, DOI: 10.1021/la040064d.
- 615 (43) Jurin, F. E.; Buron, C. C.; Magnenet, C.; Quinart, M.; Lakard, S.; Filiâtre, C.; Lakard,
616 B., Predictive tools for selection of appropriate polyelectrolyte multilayer film for the
617 functionalization of organic membranes. *Colloid. Surf. A Physicochem. Eng. Asp.* **2015**,
618 *486*, 153-160, DOI: 10.1016/j.colsurfa.2015.09.043.
- 619 (44) Song, Y. S.; Lee, J. H.; Kang, S. W.; Kim, S. W., Performance of β -galactosidase
620 pretreated with lactose to prevent activity loss during the enzyme immobilisation
621 process. *Food Chem.* **2010**, *123* (1), 1-5, DOI: 10.1016/j.foodchem.2010.04.043.
- 622 (45) Taylor, J. R., *Introduction To Error Analysis: The Study of Uncertainties in Physical*
623 *Measurements*. University Science Books: 1997.

- 624 (46) Zhuravlev, L. T., The surface chemistry of amorphous silica. Zhuravlev model.
625 *Colloid. Surf. A Physicochem. Eng. Asp.* **2000**, *173* (1), 1-38, DOI: 10.1016/S0927-
626 7757(00)00556-2.
- 627 (47) Meléndez-Ortiz, H. I.; Puente-Urbina, B.; Castruita-de León, G.; Mercado-Silva, J.
628 A.; Saucedo-Salazar, E.; García-Cerda, L. A., Covalent attachment of poly(allylamine
629 hydrochloride) onto ordered silica foams. *J. Porous Mater.* **2020**, *27* (3), 929-937, DOI:
630 10.1007/s10934-020-00870-8.
- 631 (48) Sui, C.; Preece, J. A.; Zhang, Z., Novel polystyrene sulfonate–silica microspheres
632 as a carrier of a water soluble inorganic salt (KCl) for its sustained release, via a dual-
633 release mechanism. *RSC Adv.* **2017**, *7* (1), 478-481, DOI: 10.1039/C6RA25488H.
- 634 (49) Zhao, H. C.; Wu, X. T.; Tian, W. W.; Ren, S. T., Synthesis and Thermal Property of
635 Poly(Allylamine Hydrochloride). *Adv. Mater. Res.* **2011**, *150-151*, 1480-1483, DOI:
636 10.4028/www.scientific.net/AMR.150-151.1480.
- 637 (50) Jadhav, S. A.; Nisticò, R.; Magnacca, G.; Scalarone, D., Packed hybrid silica
638 nanoparticles as sorbents with thermo-switchable surface chemistry and pore size for
639 fast extraction of environmental pollutants. *RSC Adv.* **2018**, *8* (3), 1246-1254, DOI:
640 10.1039/C7RA11869D.
- 641 (51) Chan, W. Y.; King, E. J.; Olsen, B. D., Hydrophobic and Bulk Polymerizable Protein-
642 Based Elastomers Compatibilized with Surfactants. *ACS Sustainable Chem. Eng.* **2019**, *7*
643 (10), 9103-9111, DOI: 10.1021/acssuschemeng.8b03557.
- 644 (52) Pirozzi, D.; Abagnale, M.; Minieri, L.; Pernice, P.; Aronne, A., In-situ sol-gel
645 modification strategies to develop a monolith continuous microreactor for enzymatic
646 green reactions. *Chem. Eng. J.* **2016**, *306*, 1010-1016, DOI: 10.1016/j.cej.2016.08.035.
- 647 (53) Yasar Mahlicli, F.; Şen, Y.; Mutlu, M.; Alsoy Altinkaya, S., Immobilization of
648 superoxide dismutase/catalase onto polysulfone membranes to suppress
649 hemodialysis-induced oxidative stress: A comparison of two immobilization methods.
650 *J. Membr. Sci.* **2015**, *479*, 175-189, DOI: 10.1016/j.memsci.2014.12.025.
- 651 (54) Nyanhongo, G. S.; Rodríguez, R. D.; Prasetyo, E. N.; Caparrós, C.; Ribeiro, C.;
652 Sencadas, V.; Lanceros-Mendez, S.; Acero, E. H.; Guebitz, G. M., Bioactive albumin

- 653 functionalized polylactic acid membranes for improved biocompatibility. *React. Funct.*
654 *Polym.* **2013**, 73 (10), 1399-1404, DOI: 10.1016/j.reactfunctpolym.2012.12.007.
- 655 (55) Yang, H.; Yang, S.; Kong, J.; Dong, A.; Yu, S., Obtaining information about protein
656 secondary structures in aqueous solution using Fourier transform IR spectroscopy. *Nat.*
657 *Protoc.* **2015**, 10 (3), 382-396, DOI: 10.1038/nprot.2015.024.
- 658 (56) Ciolacu, D.; Chiriac, A. I.; Pastor, F. I. J.; Kokol, V., The influence of supramolecular
659 structure of cellulose allomorphs on the interactions with cellulose-binding domain,
660 CBD3b from *Paenibacillus barcinonensis*. *Bioresour. Technol.* **2014**, 157, 14-21, DOI:
661 10.1016/j.biortech.2014.01.027.
- 662 (57) Barth, A., Infrared spectroscopy of proteins. *BBA-Bioenergetics* **2007**, 1767 (9),
663 1073-1101, DOI: 10.1016/j.bbabi.2007.06.004.
- 664 (58) Kumar, A.; Park, G. D.; Patel, S. K. S.; Kondaveeti, S.; Otari, S.; Anwar, M. Z.; Kalia,
665 V. C.; Singh, Y.; Kim, S. C.; Cho, B.-K.; Sohn, J.-H.; Kim, D. R.; Kang, Y. C.; Lee, J.-K., SiO₂
666 microparticles with carbon nanotube-derived mesopores as an efficient support for
667 enzyme immobilization. *Chem. Eng. J.* **2019**, 359, 1252-1264, DOI:
668 10.1016/j.cej.2018.11.052.
- 669 (59) Bedade, D. K.; Muley, A. B.; Singhal, R. S., Magnetic cross-linked enzyme
670 aggregates of acrylamidase from *Cupriavidus oxalaticus* ICTDB921 for biodegradation
671 of acrylamide from industrial waste water. *Bioresour. Technol.* **2019**, 272, 137-145, DOI:
672 10.1016/j.biortech.2018.10.015.
- 673 (60) Schwinté, P.; Ball, V.; Szalontai, B.; Haikel, Y.; Voegel, J. C.; Schaaf, P., Secondary
674 Structure of Proteins Adsorbed onto or Embedded in Polyelectrolyte Multilayers.
675 *Biomacromolecules* **2002**, 3 (6), 1135-1143, DOI: 10.1021/bm025547f.
- 676 (61) Puente-Santiago, A. R.; Rodríguez-Padrón, D.; Quan, X.; Muñoz Batista, M. J.;
677 Martins, L. O.; Verma, S.; Varma, R. S.; Zhou, J.; Luque, R., Unprecedented Wiring
678 Efficiency of Sulfonated Graphitic Carbon Nitride Materials: Toward High-Performance
679 Amperometric Recombinant CotA Laccase Biosensors. *ACS Sustainable Chem. Eng.*
680 **2019**, 7 (1), 1474-1484, DOI: 10.1021/acssuschemeng.8b05107.
- 681 (62) Khakshoor, O.; Nowick, J. S., Artificial beta-sheets: chemical models of beta-
682 sheets. *Curr. Opin. Chem. Biol.* **2008**, 12 (6), 722-729, DOI: 10.1016/j.cbpa.2008.08.009.

- 683 (63) Secundo, F., Conformational changes of enzymes upon immobilisation. *Chem.*
684 *Soc. Rev.* **2013**, *42* (15), 6250-6261, DOI: 10.1039/C3CS35495D.
- 685 (64) Cooper, C. L.; Dubin, P. L.; Kayitmazer, A. B.; Turksen, S., Polyelectrolyte–protein
686 complexes. *Curr. Opin. Colloid Interface Sci.* **2005**, *10* (1), 52-78, DOI:
687 10.1016/j.cocis.2005.05.007.
- 688 (65) Zhang, D. H.; Yuwen, L. X.; Peng, L. J., Parameters Affecting the Performance of
689 Immobilized Enzyme. *J. Chem.* **2013**, 1-7, DOI: 10.1155/2013/946248.
- 690 (66) Song, Y. S.; Suh, Y. J.; Park, C.; Kim, S. W., Improvement of lactulose synthesis
691 through optimization of reaction conditions with immobilized β -galactosidase. *Korean*
692 *J. Chem. Eng.* **2013**, *30* (1), 160-165, DOI: 10.1007/s11814-012-0105-1.
- 693 (67) Urrutia, P.; Bernal, C.; Wilson, L.; Illanes, A., Improvement of Chitosan
694 Derivatization for the Immobilization of *Bacillus circulans* β -Galactosidase and Its
695 Further Application in Galacto-oligosaccharide Synthesis. *J. Agric. Food Chem.* **2014**, *62*
696 (41), 10126-10135, DOI: 10.1021/jf500351j.
- 697 (68) Osman, A.; Symeou, S.; Trisse, V.; Watson, K. A.; Tzortzis, G.; Charalampopoulos,
698 D., Synthesis of prebiotic galactooligosaccharides from lactose using bifidobacterial β -
699 galactosidase (BbgIV) immobilised on DEAE-Cellulose, Q-Sepharose and amino-ethyl
700 agarose. *Biochem. Eng. J.* **2014**, *82*, 188-199, DOI: 10.1016/j.bej.2013.11.020.
- 701 (69) Karimi Alavijeh, M.; Meyer, A. S.; Gras, S.; Kentish, S. E., The role of cations in
702 regulating reaction pathways driven by *Bacillus circulans* β -galactosidase. *Chem. Eng. J.*
703 **2020**, *395*, 125067, DOI: 10.1016/j.cej.2020.125067.
- 704 (70) Cai, Z.; Wei, Y.; Wu, M.; Guo, Y.; Xie, Y.; Tao, R.; Li, R.; Wang, P.; Ma, A.; Zhang, H.,
705 Lipase Immobilized on Layer-by-Layer Polysaccharide-Coated Fe₃O₄@SiO₂
706 Microspheres as a Reusable Biocatalyst for the Production of Structured Lipids. *ACS*
707 *Sustainable Chem. Eng.* **2019**, *7* (7), 6685-6695, DOI:
708 10.1021/acssuschemeng.8b05786.
- 709 (71) Sarma, R.; Islam, M. S.; Miller, A.-F.; Bhattacharyya, D., Layer-by-Layer-
710 Assembled Laccase Enzyme on Stimuli-Responsive Membranes for Chloro-Organics
711 Degradation. *ACS Appl. Mater. Interfaces* **2017**, *9* (17), 14858-14867, DOI:
712 10.1021/acsmi.7b01999.

- 713 (72) Agrawal, D. C.; Yadav, A.; Kesarwani, R.; Srivastava, O. N.; Kayastha, A. M.,
714 Immobilization of fenugreek β -amylase onto functionalized graphene quantum dots
715 (GQDs) using Box-Behnken design: Its biochemical, thermodynamic and kinetic studies.
716 *Int. J. Biol. Macromol.* **2020**, *144*, 170-182, DOI: 10.1016/j.ijbiomac.2019.12.033.
- 717 (73) Konermann, L., Protein Unfolding and Denaturants. *eLS. John Wiley & Sons, Ltd:*
718 *Chichester* **2012**, DOI: 10.1002/9780470015902.a0003004.pub2.
- 719 (74) Zaboli, M.; Zaboli, M.; Torkzadeh-Mahani, M., From in vitro to in silico: Modeling
720 and recombinant production of DT-Diaphorase enzyme. *Int. J. Biol. Macromol.* **2020**,
721 *143*, 213-223, DOI: 10.1016/j.ijbiomac.2019.12.029.
- 722 (75) Dhiman, S. S.; Kalyani, D.; Jagtap, S. S.; Haw, J.-R.; Kang, Y. C.; Lee, J.-K.,
723 Characterization of a novel xylanase from *Armillaria gemina* and its immobilization
724 onto SiO₂ nanoparticles. *Appl. Microbiol. Biotechnol.* **2013**, *97* (3), 1081-1091, DOI:
725 10.1007/s00253-012-4381-9.
- 726 (76) Perticaroli, S.; Nickels, Jonathan D.; Ehlers, G.; Sokolov, Alexei P., Rigidity,
727 Secondary Structure, and the Universality of the Boson Peak in Proteins. *Biophys. J.*
728 **2014**, *106* (12), 2667-2674, DOI: 10.1016/j.bpj.2014.05.009.
- 729 (77) DiCosimo, R.; McAuliffe, J.; Poulouse, A. J.; Bohlmann, G., Industrial use of
730 immobilized enzymes. *Chem. Soc. Rev.* **2013**, *42* (15), 6437-6474, DOI:
731 10.1039/C3CS35506C.
- 732 (78) Keller, J.; Hartley, K., Greenhouse gas production in wastewater treatment:
733 process selection is the major factor. *Water Sci. Technol.* **2003**, *47* (12), 43-48, DOI:
734 10.2166/wst.2003.0626.
- 735
- 736

745 **Figure Captions**

746 **Figure 1.** A schematic representation of the cross-linked layer-by-layer encapsulation
747 of the enzyme onto silica particles in this study. PAH: Poly(allylamine hydrochloride),
748 PSS: Poly(styrene sulfonate). The shapes do not represent the exact particle
749 morphology, molecule sizes or interaction between different layers but provide a visual
750 guide.

751 **Figure 2.** (A) ATR-FTIR spectra of SiO₂, native enzyme and immobilized enzyme. (B)
752 Zeta potential measurements for the layer-by-layer depositions in Tris buffer at pH=7.2.
753 (C) ATR-FTIR spectrum of Amide I band for the native and immobilized enzymes.

754 **Figure 3.** (A) Poisson-Boltzmann electrostatic surface potential of the enzyme
755 estimated at pH 6 showing negatively charged regions (red), uncharged regions (white)
756 and positively charged regions (blue). (B) Free amine groups of the enzyme coloured
757 green, which can potentially react with glutaraldehyde. (C) Surface regions (yellow)
758 involved in enzyme-enzyme interactions were predicted by PSIVER (protein-protein
759 interaction sites prediction server). (D) The 3D surface structure of the enzyme
760 showing the region of its catalytic pocket (cyan). The visualization was generated using
761 Chimera software and the 3D structure was obtained from the Protein Data Bank (PDB)
762 with a code of 4ypj. Four different views of the enzyme are represented in A to C.

763 **Figure 4.** (A) time-course of the synthesis of LacNAc with the use of immobilized and
764 free enzyme at 50 °C with initial lactose and GlcNAc concentrations of 50 mM and 500
765 mM, respectively. (B) The ratio of transgalactosylation to hydrolysis rates for

766 immobilized and free enzyme. (C) The specific productivity of LacNAc after 90 min and
767 150 min of the reaction with the use of immobilized or free enzyme.

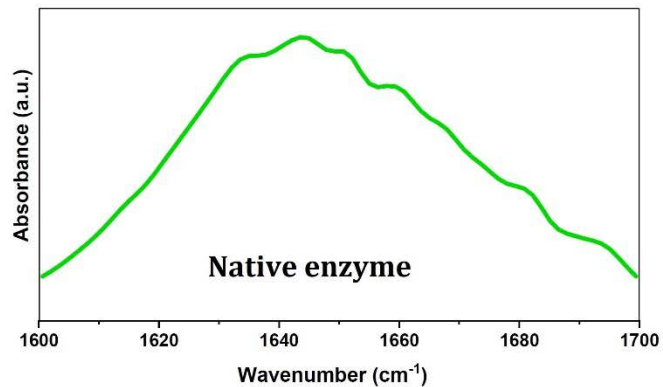
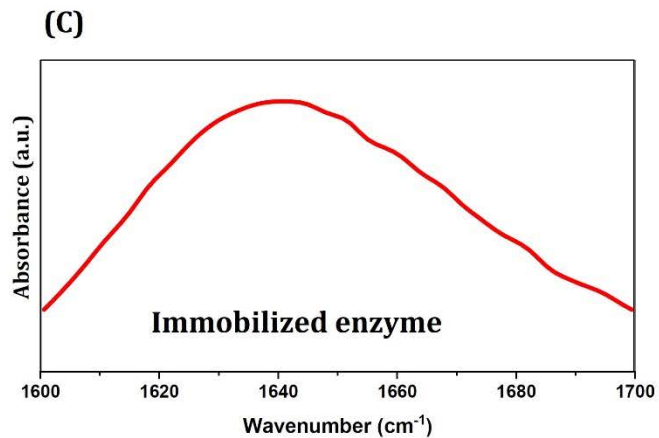
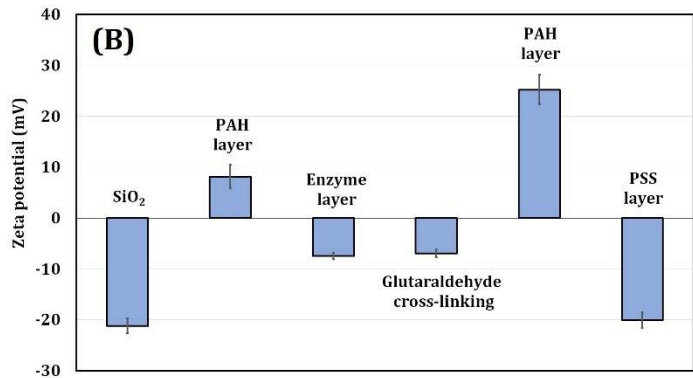
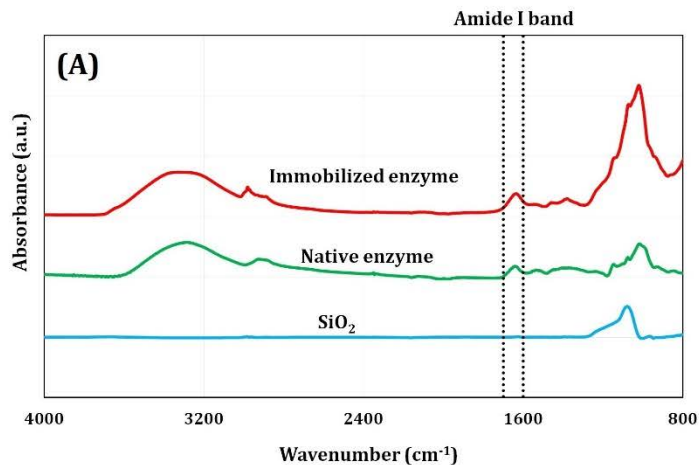
768 **Figure 5.** Natural logarithm of the residual activity of (A) the immobilized enzyme and
769 (B) the free enzyme versus incubation time at elevated temperatures. (C) Natural
770 logarithm of the thermal inactivation rate constant versus the reciprocal of the absolute
771 temperature.

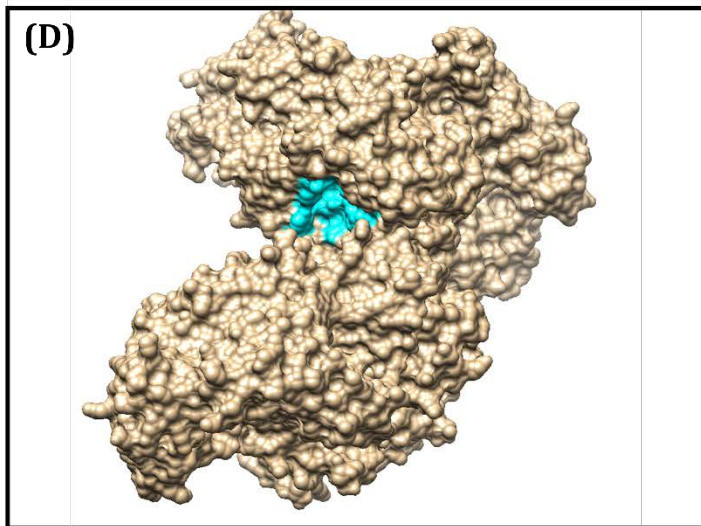
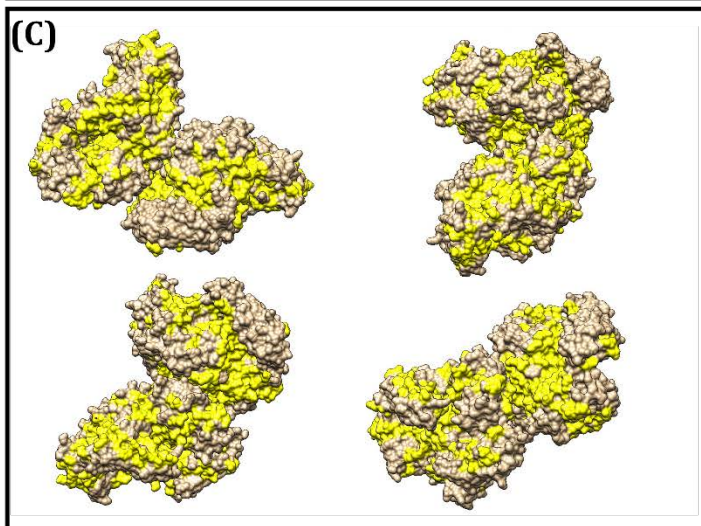
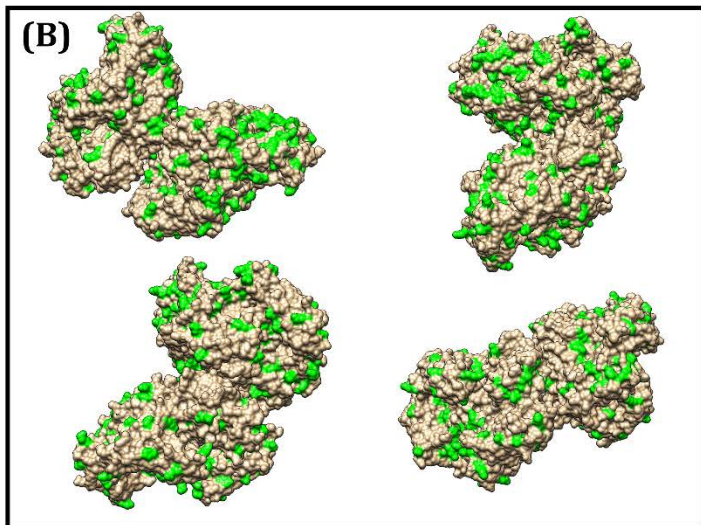
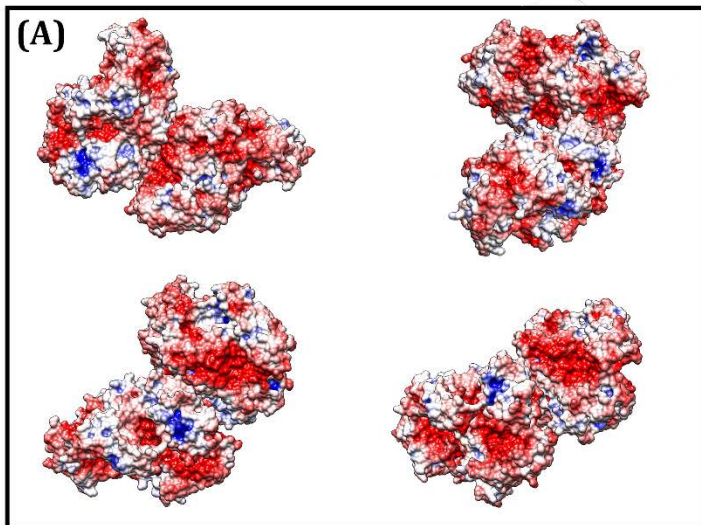
772 **Figure 6.** The transgalactosylation activity of the immobilized and free enzymes after
773 incubation for 30 min at elevated temperatures, relative to the case of the same enzyme
774 with no incubation. All activity tests were conducted at 50 °C for 10 min.

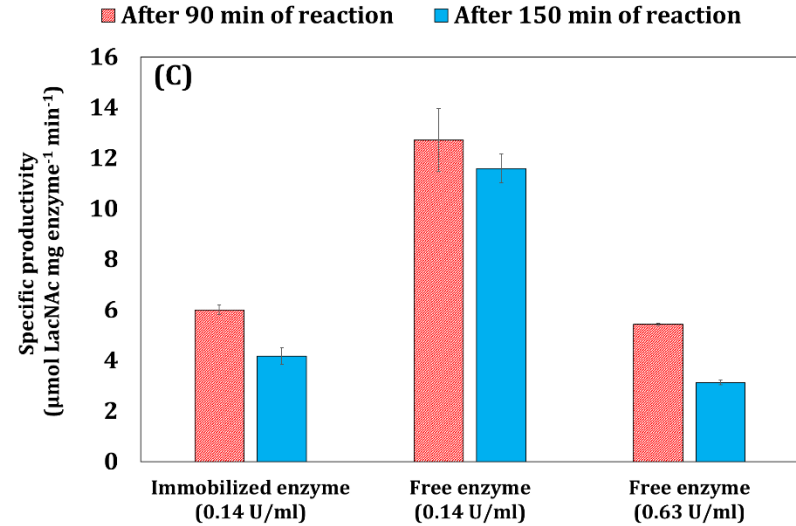
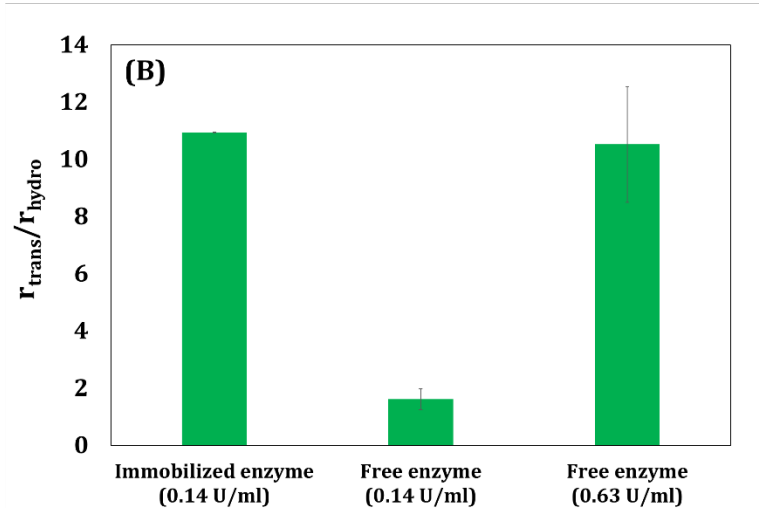
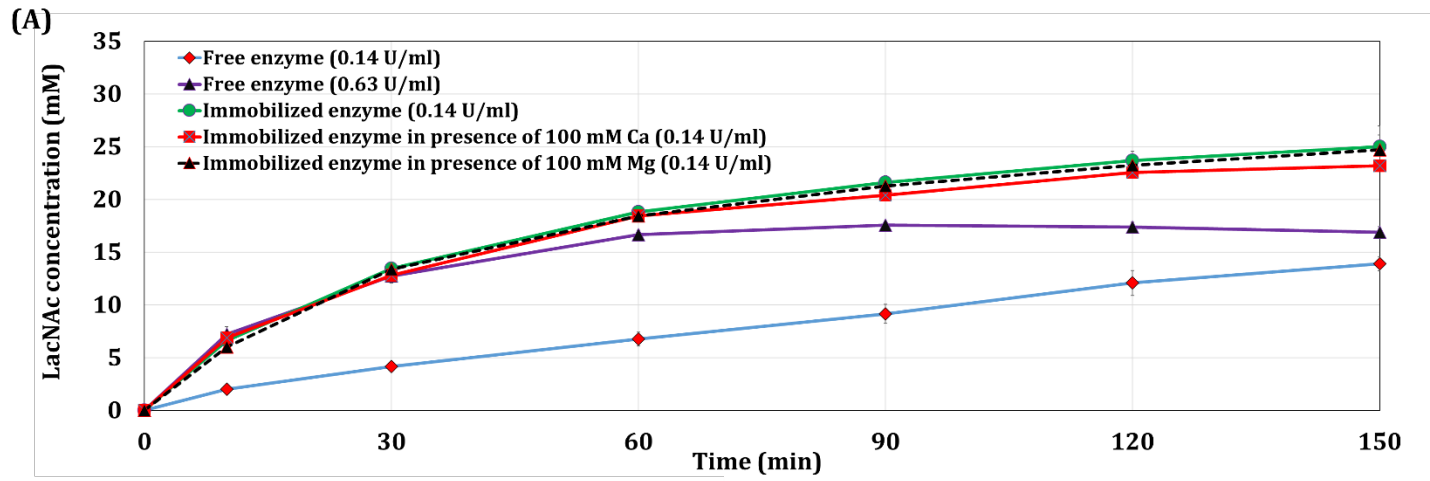
775 **Figure 7.** (A) Variations in the molar yield of LacNAc after eight reuse cycles of the
776 immobilized enzyme. (B) Changes in the profitability parameter (Net Present Value;
777 NPV) as a function of number of reuse cycles of the immobilized enzyme for a plant with
778 a downstream process based on selective crystallization. The cost parameters and
779 assumptions for the NPV calculation are described in Tables 1S and 2S in the
780 Supplementary Information.

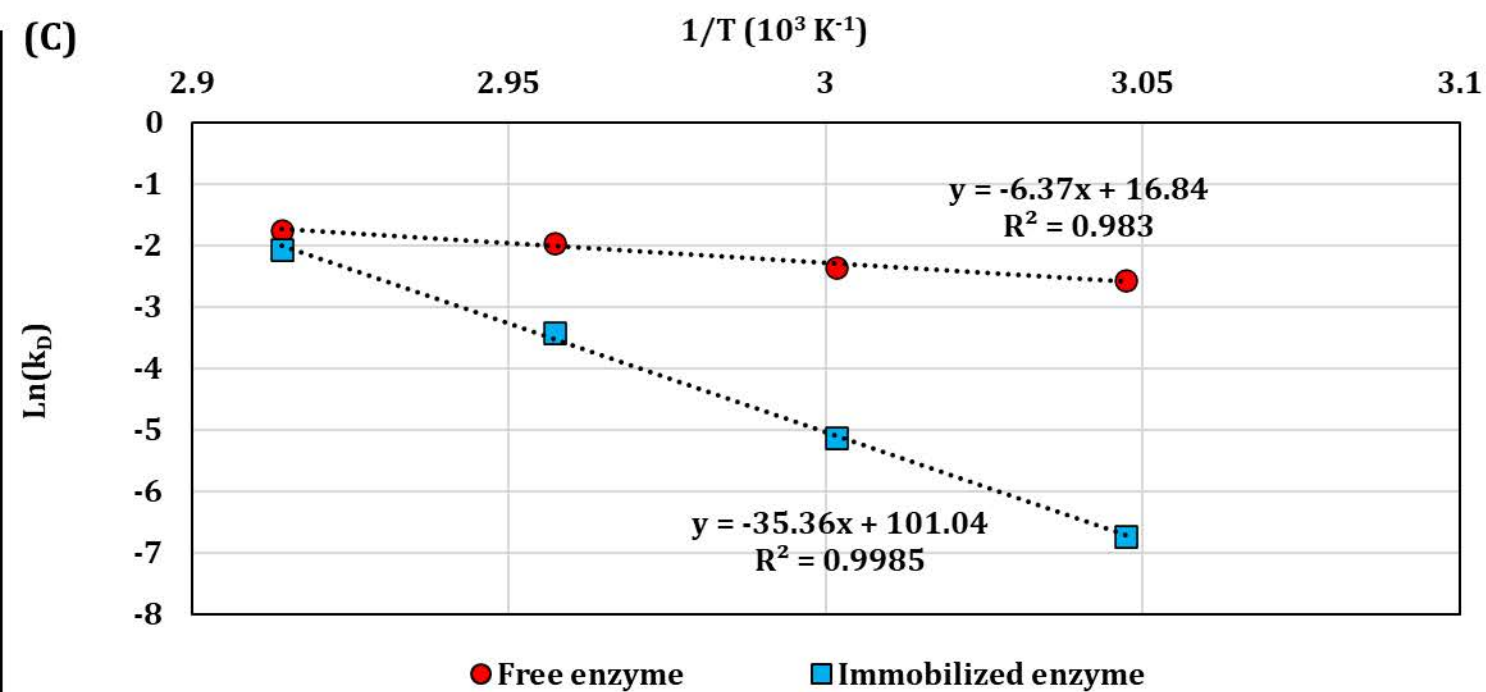
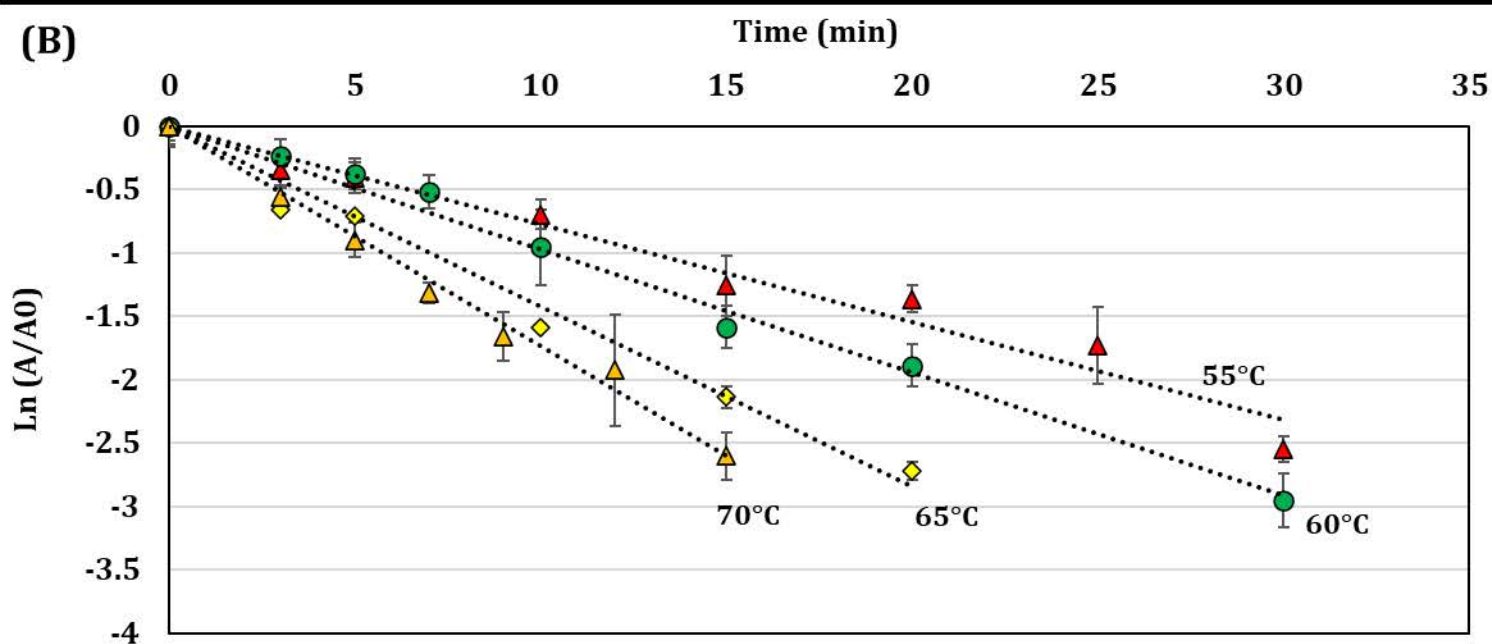
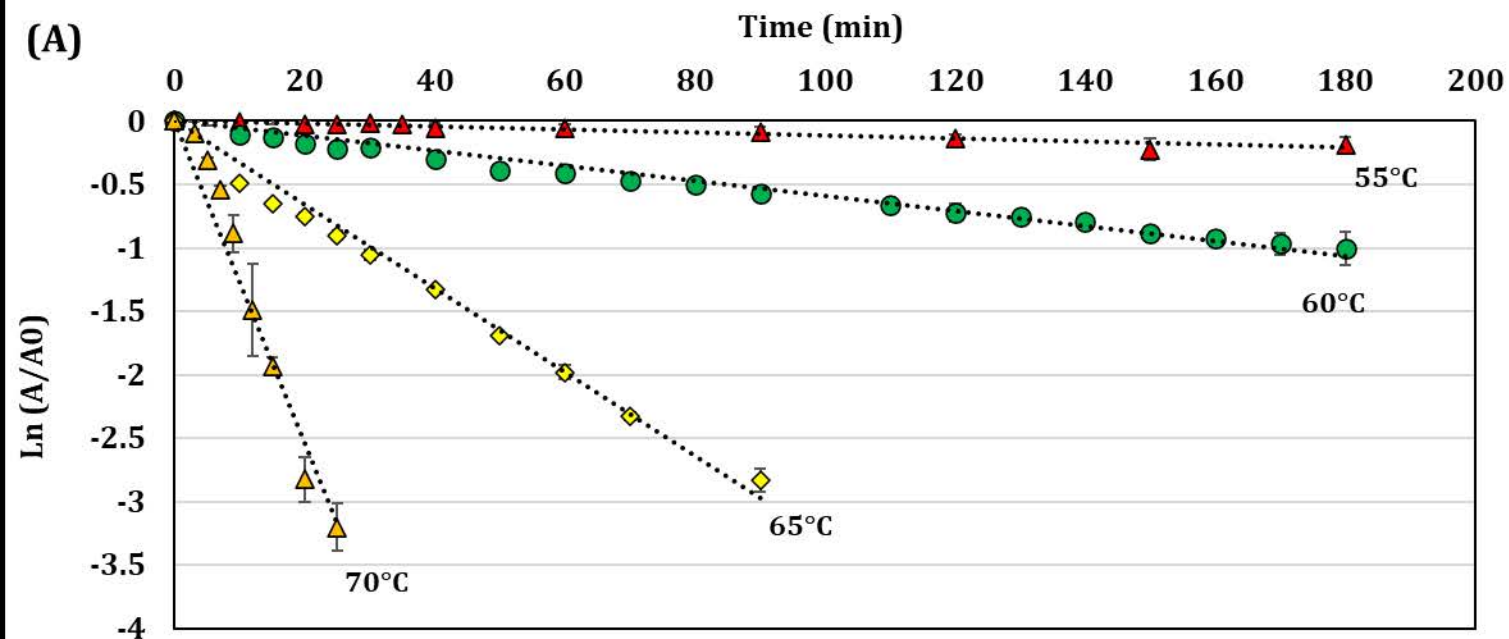
781

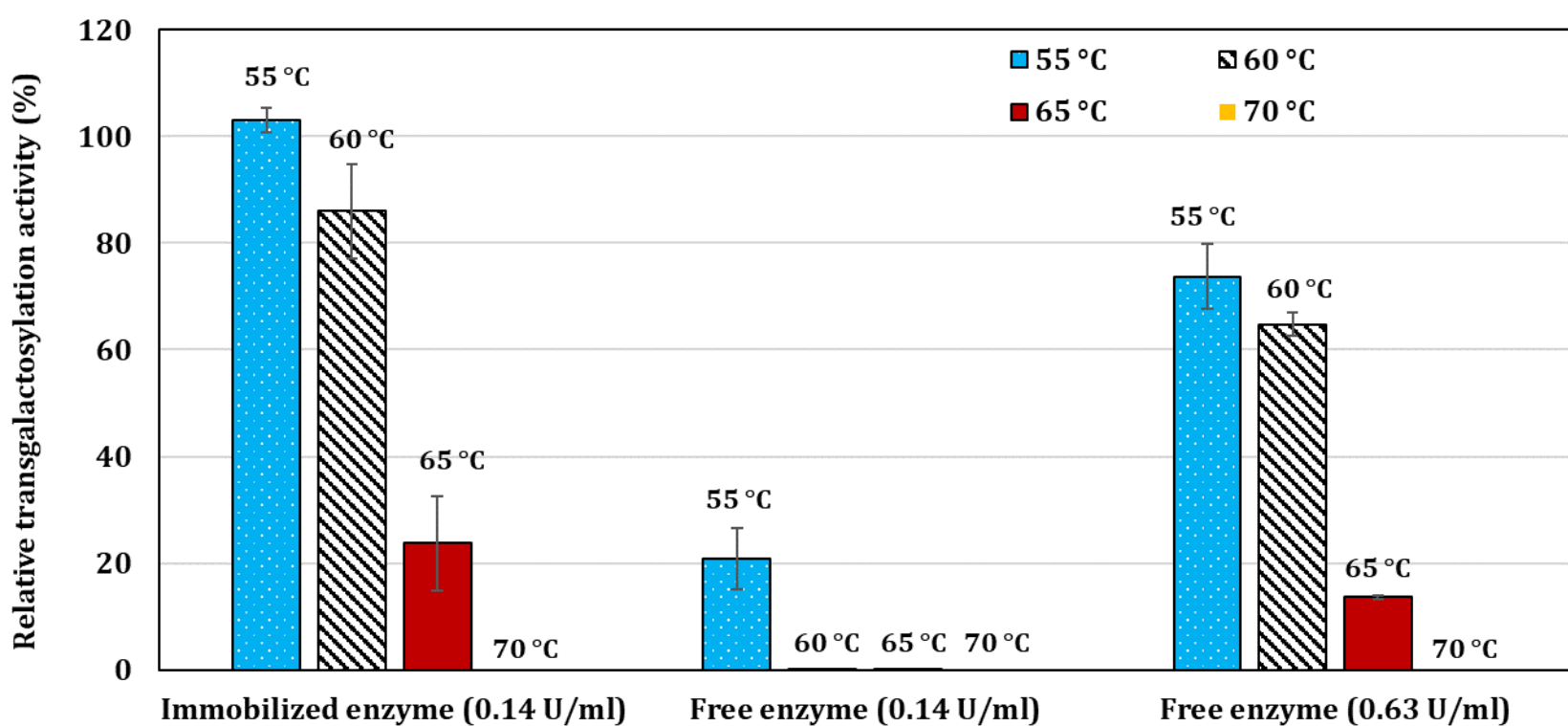
782



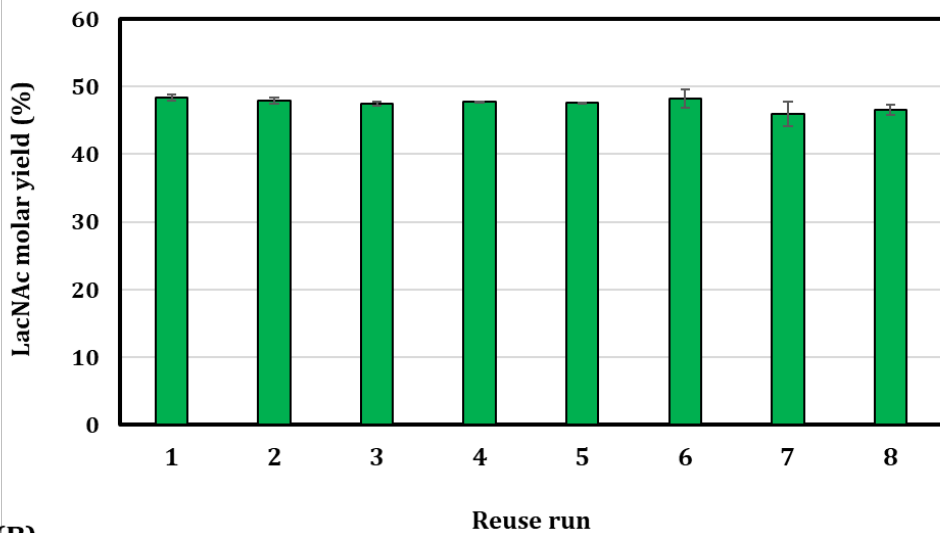








(A)



(B)

